AQUATIC CONSERVATION: MARINE AND FRESHWATER ECOSYSTEMS

Aquatic Conserv: Mar. Freshw. Ecosyst. **26** (Suppl. 2): 237–250 (2016)

Published online in Wiley Online Library
(wileyonlinelibrary.com). DOI: 10.1002/aqc.2654

Drones that see through waves – preliminary results from airborne fluid lensing for centimetre-scale aquatic conservation

VED CHIRAYATH[a,*] and SYLVIA A. EARLE[b]

[a]*Laboratory for Advanced Sensing, Earth Science Division, NASA Ames Research Center, CA, USA*

[b]*National Geographic Society and Sylvia Earle Alliance & Mission Blue*

ABSTRACT

1. The use of fluid lensing technology on unmanned aerial vehicles (UAVs, or drones) is presented as a novel means for 3D imaging of aquatic ecosystems from above the water's surface at the centimetre scale. Preliminary results are presented from airborne fluid lensing campaigns conducted over the coral reefs of Ofu Island, American Samoa (2013) and the stromatolite reefs of Shark Bay, Western Australia (2014), covering a combined area of 15 km^2. These reef ecosystems were revealed with centimetre-scale 2D resolution, and an accompanying 3D bathymetry model was derived using fluid lensing, Structure from Motion and UAV position data. Data products were validated from *in situ* survey methods including underwater calibration targets, depth measurements and millimetre-scale high-dynamic-range gigapixel photogrammetry.

2. Fluid lensing is an experimental technology that uses water-transmitting wavelengths to passively image underwater objects at high-resolution by exploiting time-varying optical lensing events caused by surface waves. Fluid lensing data are captured from low-altitude, cost-effective electric UAVs to achieve multispectral imagery and bathymetry models at the centimetre scale over regional areas. As a passive system, fluid lensing is presently limited by signal-to-noise ratio and water column inherent optical properties to ~10 m depth over visible wavelengths in clear waters.

3. The datasets derived from fluid lensing present the first centimetre-scale images of a reef acquired from above the ocean surface, without wave distortion. The 3D multispectral data distinguish coral, fish and invertebrates in American Samoa, and reveal previously undocumented, morphologically distinct, stromatolite structures in Shark Bay. These findings suggest fluid lensing and multirotor electric drones represent a promising advance in the remote sensing of aquatic environments at the centimetre scale, or 'reef scale' relevant to the conservation of reef ecosystems. Pending further development and validation of fluid lensing methods, these technologies present a solution for large-scale 3D surveys of shallow aquatic habitats with centimetre-scale spatial resolution and hourly temporal sampling.

Received 22 October 2015; Revised 04 March 2016; Accepted 12 March 2016

KEY WORDS: fluid lensing; airborne remote sensing; coastal bathymetry; coral reef; stromatolite; American Samoa; Shark Bay

*Correspondence to: Ved Chirayath, NASA Ames Research Center, Mailstop 232–22, Moffett Field, CA 94305, USA. Email: ved.chirayath@nasa.gov

INTRODUCTION

The value of Earth's aquatic environments to human survival cannot be overstated. With the evolution of oxygen-producing cyanobacterial microbes 3.5 billion years ago, microbial reefs in Earth's shallow aquatic ecosystems arguably terraformed our planet into the human life-support system it is today, fundamentally changing its atmospheric and geochemical composition in our favour (Grotzinger and Knoll, 1999; Canfield, 2005). Microbial reefs, known as stromatolites, dominate 80% of Earth's fossil record and continue to thrive today in striking abundance along Shark Bay, Western Australia (Playford *et al.*, 2013). Through the lens of such extant stromatolites, we are afforded a rare glimpse into the one of the most ancient and enduring living systems on Earth, which currently informs astrobiologists in the search for extraterrestrial life on Mars (McKay and Stoker, 1989). However, before the 2014 Shark Bay field campaign, no large-scale survey of modern stromatolites at the centimetre scale existed, severely limiting our understanding of stromatolites' morphogenesis at their relevant growth scale (Suosaari *et al.*, 2016).

By comparison, today's modern reef ecosystems, such as coral reefs, include a larger diversity of life, supporting essential biodiversity across the planet including algae, fish, sea turtles, sharks and invertebrates, among other organisms (Moberg and Folke, 1999). Just as prehistoric microbial reefs did in early Earth's history, modern coral reefs have a global distribution (Figure 1, data source (UNEP-WCMC, 2010)) and play a crucial role in regulating the planet's biosphere and supporting the activities of modern civilization (Costanza *et al.*, 1997; Ridgwell and Zeebe, 2005). At present, however, coral reefs face one of the most significant challenges in their history on Earth, triggered by unprecedented anthropogenic pressures, ocean acidification, global warming, sea-level rise, habitat destruction, agricultural runoff and overfishing, among other contributing stressors (Bellwood *et al.*, 2004). Compounding our understanding of the impacts of these emergent pressures is a severe lack of remote sensing data over regional scales regarding the resilience of coral reefs at spatial scales characteristic of their typical growth rates of ~1 cm per year (Edinger *et al.*, 2000). Such data are vital for adequate management of these aquatic resources (Bellwood *et al.*, 2004).

The need for global monitoring of reef systems is thus fundamental not only to the conservation and understanding of the extent, resilience and makeup

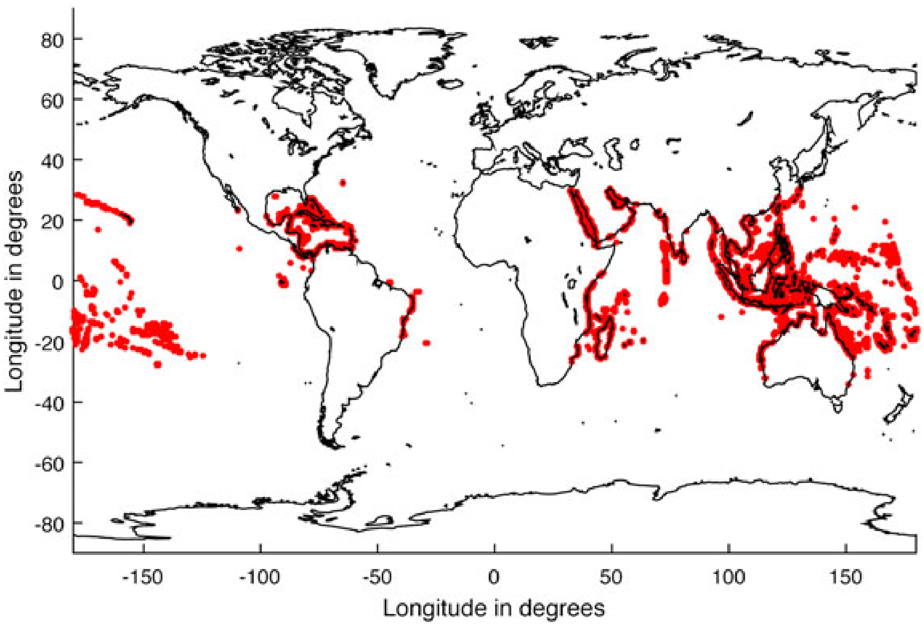

Figure 1. Global coral reef distribution as of 2010. Distribution of global, shallow, warm water coral reefs plotted in red, based on UNEP 2010 database (UNEP-WCMC, 2010).

of modern coral reefs, but also to our knowledge of the evolution of similar benthic systems on early Earth, and possibly elsewhere in the solar system, through the observation of modern stromatolite reefs. As reef systems come under pressure from rapidly changing anthropogenic impacts and climate change, observational data from remote sensing at the relevant resolution on a global scale are urgently needed to make informed policy and management decisions (Hughes *et al.*, 2003; Glover and Earle, 2004).

Standard coral reef and other shallow aquatic ecosystem remote sensing has been characterized by measurements and determination of habitat, geomorphology, water properties, bathymetry, currents and waves (Goodman *et al.*, 2013). Existing airborne and spaceborne earth science technologies specifically employ imaging spectroscopy through hyperspectral remote sensing (AVIRIS (Green *et al.*, 1998), HICO (Corson *et al.*, 2008), multispectral imaging (Landsat 8 (Roy *et al.*, 2014), WorldView-2 (Aguilar *et al.*, 2013)), and radar altimeters (JASON-1/2/3 (Bannoura *et al.*, 2005)) to study these systems. However, such instruments operate with effective spatial resolutions of 0.5–30 m (Aguilar *et al.*, 2013; Roy *et al.*, 2014). In addition, submerged objects imaged from above the ocean surface are subject to large optical distortions from refraction at the air-water interface (Martin, 2014). As a result, remote sensing systems capable of centimetre-scale spatial resolutions over land may only operate over water with an effective resolution at the metre scale, depending on the surface wave properties (Chirayath, 2014; Chirayath and Instrella, 2016).

With typical reef accretion rates ranging from 1–14 mm per year for corals (Edinger *et al.*, 2000) to ~1 mm per year for modern stromatolites (Reid *et al.*, 2000), traditional underwater surveys, photogrammetry and acoustic bottom mapping technologies remain the primary means to study these ecosystems at the centimetre scale, but are limited in spatial coverage to regions of approximately 100 m^2 (Weinberg, 1981). Consequently, shallow aquatic ecosystems remain poorly surveyed by modern remote sensing methods at the centimetre scale over regional areas.

Here, airborne fluid lensing is presented as a new remote sensing technology capable of imaging underwater marine ecosystems over regional scales from above the ocean's surface at the centimetre scale, in three dimensions. Preliminary results from two airborne fluid lensing campaigns over the coral reefs of Ofu Island, American Samoa (2013) and the stromatolite reefs of Shark Bay, Western Australia (2014) are presented as a proof of concept. These shallow reef ecosystems were successfully resolved at the centimetre scale, in 3D, using fluid lensing by post-processing high-frame-rate image data with validation by *in situ* underwater measurements. Although still under active development, experimental fluid lensing technology may present a valuable and cost-effective tool for shallow marine conservation, pending further development and validation.

METHODOLOGY

Two experimental airborne surveys were conducted over the coral reefs of Ofu Island, American Samoa (2013) and the stromatolite reefs of Shark Bay, Western Australia (2014), a UNESCO World Heritage Site. The goal of the airborne campaigns was to validate fluid lensing's ability to reconstruct submerged targets in 3D from an airborne platform over unique aquatic ecosystems with diverse fluid properties. A UAV electric quadcopter platform was custom-built to host a nadir-pointing high-frame-rate video camera, relay synchronized position data and survey a region with sequential flights, each up to 20 min in duration. Videos frames were sorted into 120-frame bins and processed using the experimental fluid lensing algorithm (Chirayath, 2014) to remove refractive distortions caused by ambient surface waves. The corrected images and UAV position data were used as input frames for Structure from Motion (SfM) (Tomasi and Kanade, 1992; Kanade and Morris, 1998) to produce 2D, centimetre-scale orthophotos and a dense 3D bathymetry model. Calibration targets were distributed at varying water depths for georeferencing and bathymetry validation. Finally, terrestrial and mm-scale underwater gigapixel photogrammetry was performed to calibrate and verify 2D fluid lensing reconstructions from airborne data, perform georectification and validate derived 3D bathymetry products. It should be noted that this paper presents preliminary results from an experimental fluid lensing algorithm. Further methodology, validation and analysis of these data will be presented in forthcoming publications.

Fluid lensing imaging technology

Fluid lensing is an experimental remote sensing technology under active development (Chirayath, 2014; Chirayath and Instrella, 2016) designed to image submerged objects in the presence of surface waves. As a passive remote sensing technology, it is limited by the inherent optical properties of the water column and ambient irradiance to depths of ~10 m in clear natural waters. Fluid lensing passively images underwater objects over water-transmitting wavelengths by exploiting time-varying optical lensing events caused by refractive distortions arising from travelling surface waves over the ocean. Fluid lensing combines a theoretical model and algorithm for opto-fluidic interactions at the fluid surface boundary with unique hardware and computational imaging to remove strong distortions along the optical path (Figure 2) and enhance the signal-to-noise ratio (SNR) and angular resolution of an otherwise aperture-constrained optical system and focal plane array.

In the case of remote sensing of the Earth's ocean, certain surface waves have a favourable curvature and displacement that causes a momentary optical magnification of an underwater target. Such events commonly occur when a wave crest travels over a region. Conversely, when a wave trough passes over a region, a net optical demagnification is observed. The approximate regime of ocean waves for which such favourable fluid lensing events occur is predominantly wind-driven and evolves on periods of 0.1–10 s, within the duration of an aircraft or satellite overpass (Figure 3, data source (Holthuijsen, 2010)).

By observing this regime of surface waves over a submerged target, it is possible to determine the stochastic, time-averaged wave field parameters

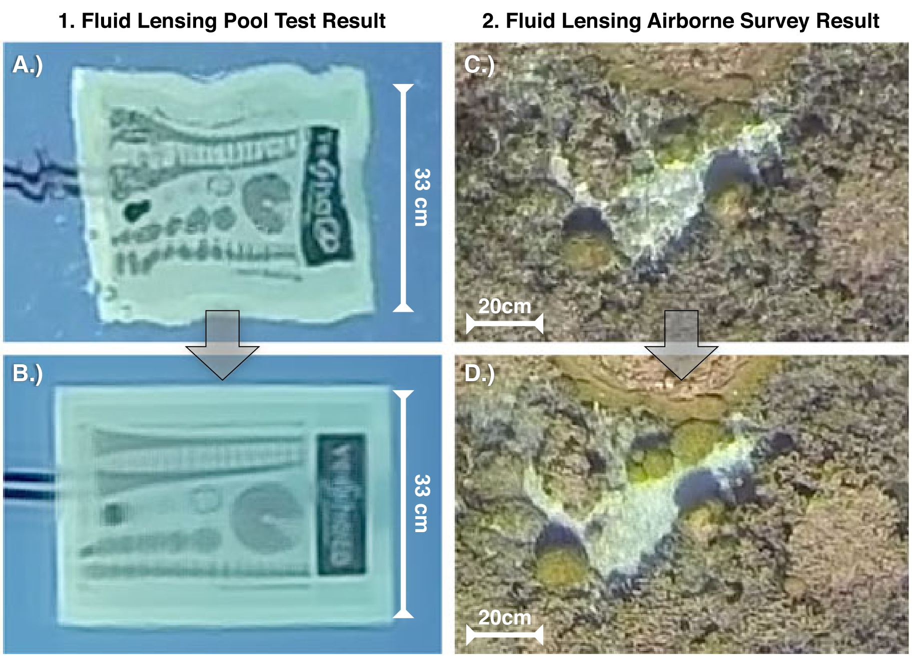

Figure 2. Preliminary fluid lensing results. (1) Fluid lensing reconstruction test in Olympic Pool with test target at 3.7 m depth, imaged from 3.5 m altitude. (A) Raw frame showing characteristic refractive distortions from surface waves, (B) reconstructed image using fluid lensing from less than 1 s of frame data. (2) Fluid lensing imaging results from Samoa survey captured from UAV at 23 m altitude, maximum depth of 2.8 m. (C) Raw frame from aerial data, (D) reconstructed image using fluid lensing from less than 1 s of frame data.

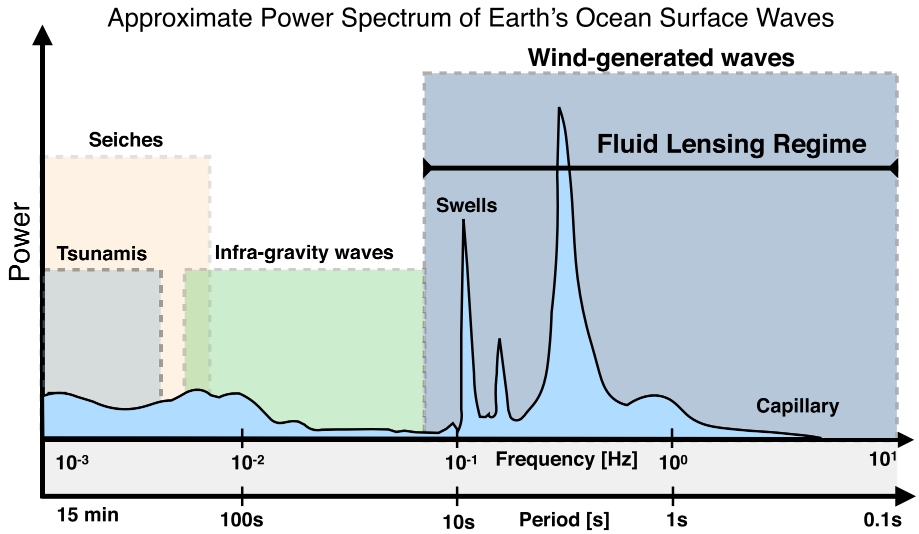

Figure 3. Fluid lensing wave regime in context of approximate power spectrum of Earth's ocean surface waves. For the experimental airborne campaigns in Samoa and Shark Bay, wave periods of 0.1–2 s were the dominant wave periods used for fluid lensing. These wave periods were chosen based on frequency of lensing events from observed wave conditions and determined groundspeed velocity of the UAVs.

using position data and high-frame-rate uncompressed video frames, captured at 60 hz or higher. Fluid lensing derives a power spectrum representation of the wave field from image data to preferentially exploit positive magnification events from instantaneous surface waves. These products are then used to reconstruct a 2D target, without refractive distortions, from a set of input frames (Figure 2). By inferring a stochastic wave model over a region from image data, fluid lensing also creates a depth estimate from the wave field and combines the result with the 2D reconstruction, UAV position data and SfM algorithms to generate a high-resolution 3D model of a scene underwater (Figure 4). All data presented were processed in part using the high-performance computing facilities of the NASA Earth Exchange (NEX). Further details and validation of the fluid lensing algorithm will be presented in forthcoming publications.

Unmanned aerial vehicles for fluid lensing

UAVs offer a cost-effective tool for high temporal and spatial remote sensing of terrestrial environments (Harwin and Lucieer, 2012), however, using UAVs for fluid lensing over aquatic environments requires unique hardware and

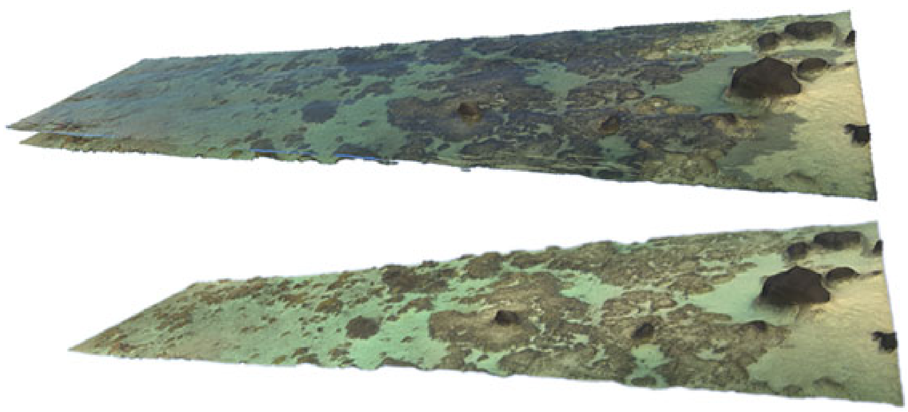

Figure 4. Fluid lensing wave field estimation and reconstruction of flight transect from American Samoa. The top figure shows the optical distortion at the air–water boundary caused by refraction from the surface wave field over a coral reef transect. The data shown are from the Samoa fluid lensing airborne campaign with fluid parameters derived from fluid lensing. The bottom figure shows the fluid lensing and SfM derived 3D reconstruction without the surface wave field distortion. Rendered in Blender on NASA Earth Exchange (NEX) supercomputer.

specialized flight operations. For the airborne survey in Samoa (2013), an electric UAV quadcopter platform was custom-built to host a nadir-pointing high-frame-rate video camera and relay synchronized position data while surveying a region with sequential flights, each up to 20 min in duration (Figure 5). Flights were conducted at between 1 and 6 m s^{-1} groundspeed as a function of observed ocean surface wave conditions, corresponding to the dominant lensing wave period (Figure 3) in order to capture sufficient lensing events for target reconstruction. The airborne survey in Shark Bay (2014) used a higher-endurance quadrotor platform to gather data. All UAVs were launched and landed under manual control, and conducted imaging transects under automated waypoint navigation. The aircraft were flown within line of sight, with a live telemetry link to ground stations. All flights were conducted between 23 and 34 m altitude, as measured by pressure-corrected GPS. Design characteristics of each UAV, specific to the operational environment, included low noise levels (<40 dB), battery-electric operation, custom marinized parts, camera gimbal pointing accuracy <0.1 degree, and a system cost under US$10 000 each.

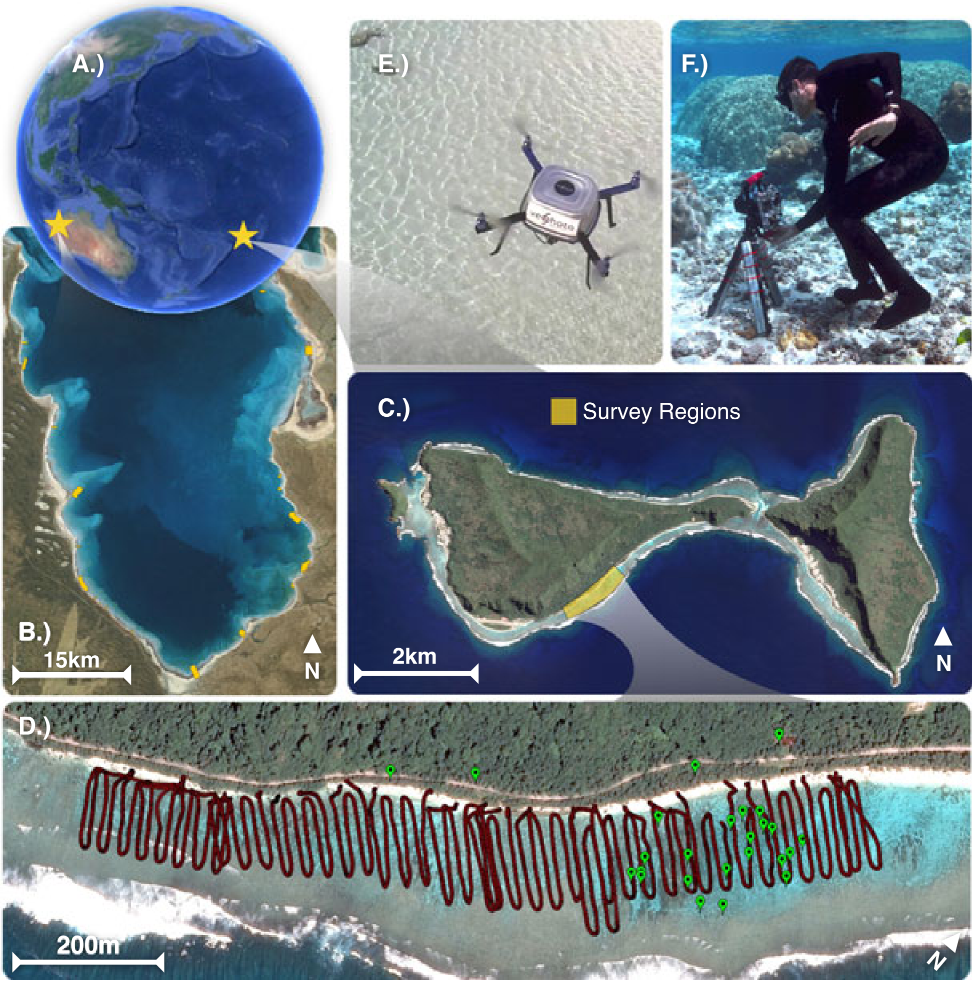

Figure 5. Survey areas and methods. (A,B.) Survey regions along Ofu Island, American Samoa and Shark Bay, Western Australia are shown in yellow and cover a combined area of ~15 km^2. (B) Survey areas distributed in Shark Bay cover ~14 km^2. (C) Survey area in Ofu Island spans 1 km^2. (D) UAV flight GPS data from airborne survey are shown in red. Photogrammetry and calibration locations are indicated by green points. The 'lawnmower' flight path was chosen to maximize 3D sampling and dwell time for fluid lensing reconstruction. (E) Custom UAV used in American Samoa field campaign shown in flight as imaged from second UAV. (F) Performing underwater gigapixel HDR photogrammetry with custom underwater nodal point imaging system.

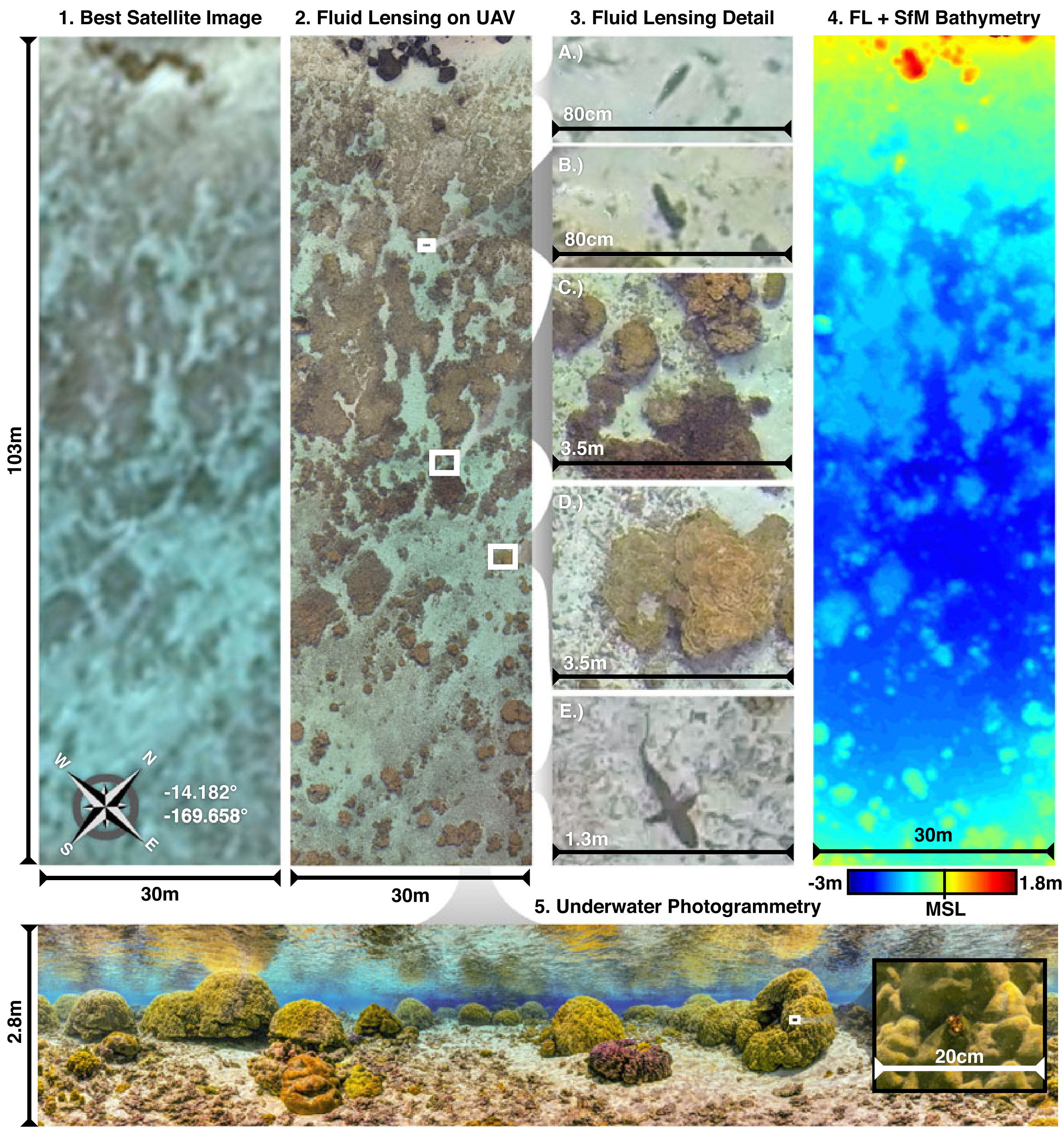

Figure 6. Preliminary American Samoa fluid lensing results. (1) Highest-resolution publicly available image of transect area captured June 2015 from Pleiades-1A satellite with 0.5 m GSD. (2) Fluid lensing processed 2D reconstruction as captured from UAV at 23 m altitude with estimated 0.5–3 cm effective spatial resolution. (3) Inset details in fluid lensing 2D reconstruction include (A) parrotfish ~20 cm in length, (B) sea cucumber ~21 cm in length, (C,D) multiple coral genera including *Porites* and *Acropora,* and (E) shark. (4) High-resolution bathymetry model generated with fluid lensing (FL) and Structure from Motion (SfM) algorithms, validated by underwater photogrammetry. Maximum depth in model is ~3 m, referenced to mean sea level (MSL). (5) Underwater gigapixel high-dynamic-range equirectangular panorama with maximum depth of 2.8 m, and inset showing mm-scale features.

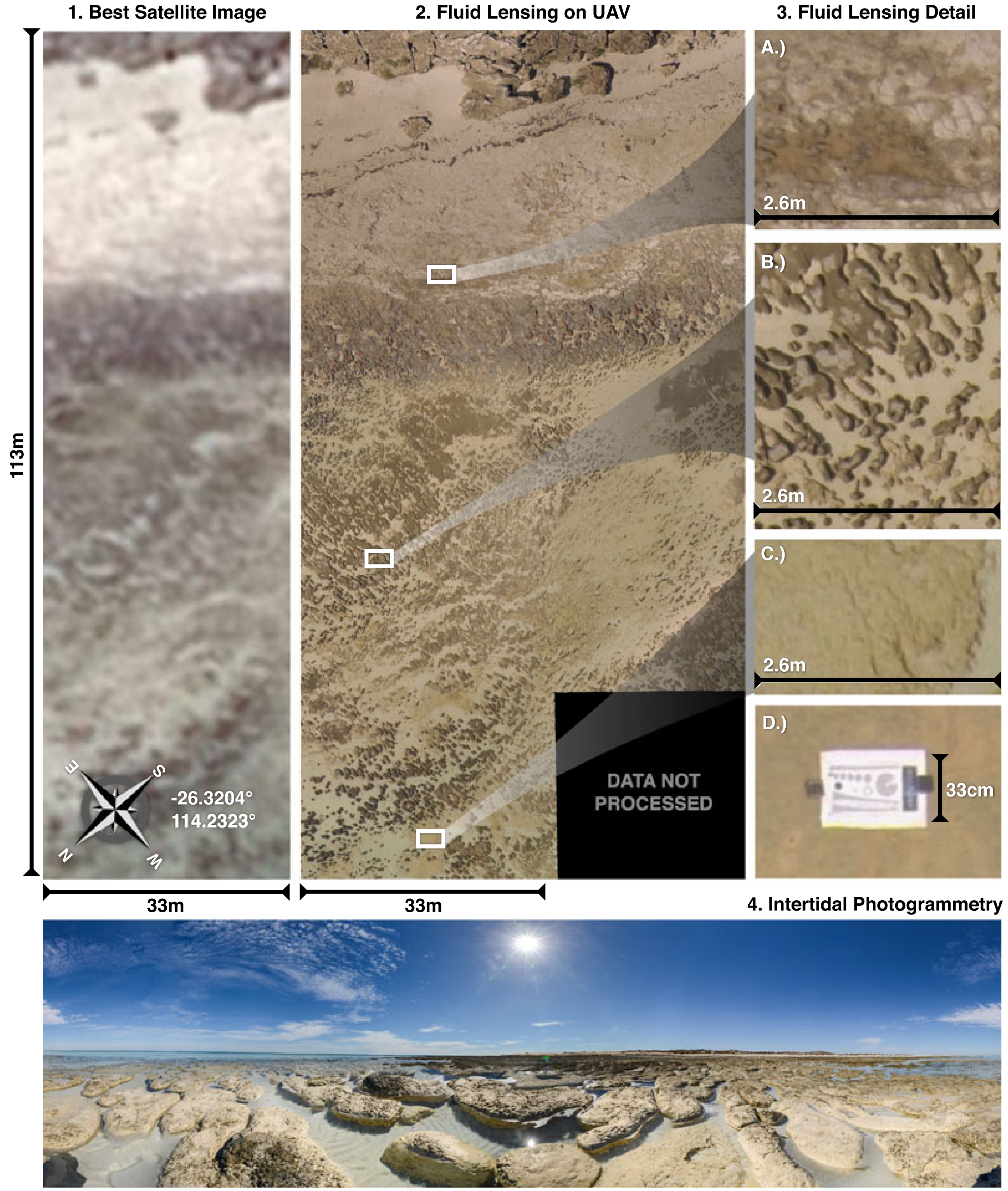

Figure 7. Preliminary Shark Bay fluid lensing results. (1) Highest-resolution publicly available image of transect area captured June 2015 from Pleiades-1A satellite with 0.5 m GSD. (2) Fluid lensing processed 2D reconstruction as captured from UAV at 33 m altitude with effective spatial resolution of 1–4 cm. (3) Detail in fluid lensing 2D reconstruction include (A) eroded stromatolite structures, (B) extant stromatolite structures, and (C) microbial mats. (D) Inset of test target in field transect at 1 m depth. (4) Photogrammetry of intertidal zone used in validation and georectification of (2).

Calibration, validation, georeferencing, and gigapixel high-dynamic-range underwater photogrammetry

Calibration and validation of fluid lensing 2D reconstruction, colour correction and 3D bathymetry products were the primary goals of the experimental airborne field campaigns. To validate 2D and 3D data generated by fluid lensing and SfM, high-resolution underwater panoramas were taken throughout both survey regions and quantitatively compared with fluid lensing reconstructions (Figure 5). For the survey regions, the highest-resolution publically available imagery identified was from the Pleiades-1A satellite with a GSD of 0.5 m, accessed June 2015 (Google, 2015a, b). Each panorama was digitally synthesized using a high-dynamic-range process (Debevec and Malik, 1997; Brown and Lowe, 2007) with thousands of images spread across the full 360° field of view from a custom underwater camera system imaging at the nodal point of a 36-megapixel digital single-lens reflex (DSLR) camera. Camera calibrations for the fluid lensing cameras and DSLR were used to compute calibration parameters for the fluid lensing and SfM algorithms, as well as photogrammetry and bathymetry scaling. Final gigapixel panoramas were produced with equirectangular and stereographic projections, geotagged control points, and instantaneous depth measurements by plumb-bob (±0.1 m). In select regions of the aerial survey results, final panoramas were further referenced as underwater survey transects for aquatic species identification (Figure 6). Finally, underwater calibration targets (Figure 7) were used to further validate reconstruction results, perform colour correction and improve accuracy of georectification.

Survey areas and airborne field campaigns

The first experimental airborne fluid lensing field campaign was part of an expedition to American Samoa's Ofu island, home to a diverse fringing reef system (Birkeland *et al.*, 2008). The survey spanned a region covering approximately 1 km^2 (Figure 5). Twenty-eight flights were conducted in August 2013, each lasting 10–20 min. Vertical take-offs and landings were performed from the shore.

The second field campaign was conducted in Shark Bay, Western Australia, home to the world's most extensive modern stromatolite system (Burns *et al.*, 2004). This survey region included multiple locations across the large hypersaline pool (Figure 5). A total of 278 flights were conducted in April 2014, each lasting 15–21 min with at least three ground control point tiles distributed in each flight area, spanning a combined survey area of approximately 14 km^2. The test target, shown in Figure 2 and Figure 7, was placed at multiple depths and locations in the survey area to gather data for fluid lensing validation. In addition, extensive *in situ* mapping and analysis were performed in the survey areas as part of a multi-scale mapping effort (Suosaari *et al.*, 2016). Owing to the remote locations of many survey areas, many flights were conducted from a survey vessel.

RESULTS

The preliminary results from the two field campaigns, displayed in Figures 6 and 7, present the first centimetre-scale image of a reef, without surface wave distortion, using fluid lensing from an unmanned aircraft. The 3D multispectral data distinctly show coral, fish and invertebrates in American Samoa (Figure 6) and reveal previously undocumented morphologically distinct stromatolite structures in Shark Bay (Figure 7). Bathymetry models produced using fluid lensing and SfM show 3D features to 5 cm in size at 3 m depth (Figure 6). The fluid lensing method described here increases the resolution of current state-of-the-art remote sensing imagery and bathymetry models, limited to 0.5–30 m resolution (Jahnert and Collins, 2012; NOAA, 2012), by up to two orders of magnitude.

Figure 6 compares preliminary results from the August 2013 Ofu Island, American Samoa field campaign with 0.5-metre imagery accessed June 2015 by the Pleiades-1A satellite (Google, 2015b). Pleiades-1A provides the highest-resolution imagery that is publicly available (Gleyzes *et al.*, 2012). A series of insets in Figure 6 from the 2D fluid lensing reconstruction resolve bleached coral from living coral, as well as coral genera including *Porites* and *Acropora* spp., in addition to a parrotfish, a shark, and a sea cucumber, at the centimetre scale in depths up to 3 m. There is no publicly available sub-metre-scale bathymetry model of the region, the best being a LIDAR survey at the metre scale (NOAA, 2012). Therefore, underwater photogrammetry with concurrent depth measurements were used to validate the fluid lensing bathymetry results. Further validation of the bathymetry model will be dependent upon future validation efforts from the area. The pre-processed uncompressed Samoa dataset is ~730GB, consisting primarily of high-frame-rate video frames. The fully post-processed uncompressed fluid lensing data, 2D and 3D results are ~5.8 TB for a region spanning ~1 km^2.

Figure 7 shows preliminary airborne fluid lensing results from the April 2014 Shark Bay field campaign compared with Pleiades-1A imagery accessed June 2015 (Google, 2015a). Here, the data resolve diverse and complex extant stromatolite structures and microbial surface mats. The preliminary datasets from the field campaign were used across Shark Bay as part of a multi-scale survey, including extensive *in situ* mapping, to study previously undocumented morphologically distinct stromatolite structures across eight ‘Stromatolite Provinces’ in Shark Bay (Suosaari *et al.*, 2016). The pre-processed compressed dataset is ~5.9 TB. The full 2D reconstruction is still being processed, but is expected to grow to ~60 TB, compressed, for the entire 14 km^2 survey. All experimental data products, including orthophotos and bathymetry models, are publicly available for download as they become available from the NASA Fluid Lensing homepage in JPEG, GeoTIFF, KMZ and KML formats.

DISCUSSION

To address the challenges of monitoring global shallow marine environments in a changing climate, there is an immediate need to develop and validate cost-effective earth science instruments capable of understanding reef ecosystems at a spatial scale relevant to their growth rate (Mumby *et al.*, 2004). We posit that this ‘reef scale’ is in the order of the annual growth rate of reef ecosystems, namely the centimetre scale for coral reefs and sub-centimetre scale for microbial reefs. These preliminary results suggest fluid lensing and multirotor electric UAVs present a promising advance in the remote sensing of aquatic ecosystems at the reef scale, offering a cost-effective solution for large-scale surveys of shallow marine habitats, pending further development and validation of the experimental fluid lensing technology.

Analysis of shallow marine ecosystems with high spatial resolution at the reef scale may translate into the capability to detect changes within an environment, such as coral bleaching, on shorter temporal scales. Consequently, the environmental effects of such events may be measured before a major event growing to regional scales for detection by existing satellite remote sensing methods at the metre scale and larger. Indeed, the technologies presented here enable finer temporal sampling at the reef scale, at whatever timescales are needed to resolve changes in the environment, as opposed to the fixed-interval sampling of satellite remote sensing data. Fluid lensing with multirotor UAVs can offer temporal resolution in the regime of 20 min for small regions and daily repeats for regions up to a square kilometre in size, with centimetre-scale spatial resolution. In the context of aquatic conservation, the enhanced temporal sensitivity of such an ‘early warning system’ may prove to be a crucial tool for determination of ecosystem stressors and their spatial and temporal dynamics (Purkis and Riegl, 2005), with the potential for mitigation and improved ecosystem management.

For coral reefs, such as those surveyed in American Samoa, remote sensing at the reef scale could improve the assessment of coral reef resilience (Rowlands *et al.*, 2012) through enhanced delineation in the mapping of species, functional diversity, geographic ranges, and connectivity. Finer spatial resolution would also augment our understanding of the community dynamics of coral ecosystems and morphological patterns on multiple scales (Purkis *et al.*, 2007). Finer spatial and temporal resolution also allows data collection at scales relevant to fish, and would thereby improve data collection on reef fish diversity, as well as the abundance and diversity of their preferred habitats (Purkis *et al.*, 2008). Finally, at an event scale, airborne fluid lensing can be particularly useful for rapid coastal surveys and change detection to document the effects of a particular tsunami, storm, or pollution, or coral bleaching event (Joyce *et al.*, 2009).

For microbial reefs, such as those surveyed in Shark Bay, remote sensing with fluid lensing at the reef scale was used to reveal morphologically distinct, and previously undocumented, stromatolite structures across eight new ‘Stromatolite Provinces’ in the hypersaline waters of Hamelin Pool, Shark Bay (Suosaari *et al.*, 2016). This multi-scale survey afforded a valuable insight into modern analogues for benthic systems on early Earth and may inform the search for hypothesized fossilized or living extra-terrestrial microbial ecosystems in Mars’ analogous hypersaline aquatic past (McKay and Stoker, 1989; Baker, 2006). Indeed, remote sensing at the reef scale may significantly enhance our understanding of biotic self-organization on large scales (Schlager and Purkis, 2015) and better guide our exploration of the solar system for extra-terrestrial life.

The preliminary data also present a new means to generate bathymetry models at the reef scale. This can be particularly useful for environments where bathymetric data cannot be collected by sonar systems from large research vessels, while avoiding problems with bathymetric data collected by water-penetrating LIDARs subject to distortions by surface wave refraction at the metre scale (NOAA, 2012). The high-resolution bathymetry models produced using airborne fluid lensing and SfM can also reduce error in physical oceanographic models of flow over reef systems (Monismith, 2007), improving models of coastal zones, flood zones, pollutant transport and the spatial extent of harmful algal blooms. Such models could be coupled to flow simulations and used to inform how best to protect the coastal cities and infrastructure from storm events (Spurgeon, 1992). Finally, reef-scale 3D imagery can also improve our ability to quantify 3D ecological characteristics of coral reefs and improve our capacity to monitor changes in the health and function of coral reef ecosystems at an ecologically relevant scale (Burns *et al.*, 2015).

While remote sensing at the centimetre scale with airborne fluid lensing can provide a wealth of useful information, it does, however, present unique challenges in terms of environmental and weather conditions, data management and computational complexity. As a passive remote sensing technology, fluid lensing is presently limited by the inherent optical properties of the water column, surface wave conditions and ambient irradiance. Absorption, scattering and reflection along the optical path limit SNR while non-linear and capillary surface waves introduce requirements for slower flight times, higher instrument sampling rates and increased computation for the same centimetre-scale reconstruction. At present, airborne fluid lensing shows applicability to imaging in depths of ~10 m under favourable surface wave conditions in clear natural waters. In addition, the processing of centimetre-scale imagery over large regional areas introduces computational challenges. The preliminary results presented show fluid lensing produces 2D imagery at a data density of ~6 TB km^{-2}, growing to approximately 60 TB km^{-2} with full-resolution 3D bathymetry data. Using a modern 1 TFLOP multicore desktop computer, the present ratio of airborne flight time to fluid lensing and SfM reconstruction is ~1:80. Consequently, to more efficiently survey large areas with these methods and perform analyses on the data products requires high-performance and high-bandwidth computational resources. Therefore, the preliminary data presented here were processed in part using the high-performance supercomputing facilities of the NASA Earth Exchange (NEX).

Lastly, understanding reef-scale conservation parameters (Horning *et al.*, 2010) over such large datasets using increased spatial and temporal resolution, RGB colour imagery, and bathymetry, will motivate the development of unique computational toolboxes and remote sensing analysis techniques. Growth in computational power and storage capacity, concurrent with the development of improved machine learning algorithms and semi-automated classification methods (Saul and Purkis, 2015), suggest that the conservation of marine ecosystems will be significantly enhanced by the acquisition of reef-scale remote sensing from airborne fluid lensing. These data can be used to improve accuracy in determining coral reef resilience, percentage cover, morphology and species abundance and distribution. Recent work applying machine learning approaches to such datasets show that centimetre-scale 3D imagery (Burns *et al.*, 2015) and 2D imagery (Beijbom *et al.*, 2015) afford significant improvements in the quantification of reef rugosity and morphology as well as ecological assessment, such as the automated annotation of benthic surveys and identification of coral species.

In conclusion, the preliminary results from airborne fluid lensing campaigns in American Samoa and Shark Bay represent a promising advance in the remote sensing of aquatic ecosystems, particularly coral reefs and microbial reefs. Together with multirotor electric UAVs, fluid lensing offers a cost-effective solution for large-scale surveys of shallow aquatic habitats and a powerful new tool for reef-scale aquatic conservation with centimetre-scale resolution in three dimensions. Further investigation is needed to fully understand the operational regimes and reconstruction accuracy of airborne fluid lensing as a function of inherent optical properties of the water column, surface wave fields, and ambient irradiance conditions. However, the preliminary results clearly indicate a step forward in our observational capacity and future understanding of aquatic ecosystems. We hope airborne fluid lensing will add new perspectives to the field of aquatic conservation.

FUTURE WORK

Fluid lensing is an experimental technology under active development, validation and testing at the NASA Ames Laboratory for Advanced Sensing. Following the field campaigns described here, fluid lensing instruments, called FluidCams, were developed with support from NASA's Earth Science Technology Office. The FluidCams specifically address the bandwidth, SNR and computational requirements of fluid lensing from UAVs and space-based platforms. FluidCam1 and FluidCam2 are custom-designed integrated optical systems, imagers and high-performance computational instruments designed for UAVs and eventual suborbital deployment. They were recently matured from NASA Technology Readiness Level (TRL) 2 to TRL 6 for operational missions on UAVs (Mai, 2015). FluidCam1 and FluidCam2 operate at image frame rates up to 1200 Hz and with data rates exceeding 370MB/s. These capabilities enable sub-centimetre fluid lensing reconstructions. In addition, the FluidCams communicate directly to the UAV autopilots and modify the flight speed depending on observed ocean wave conditions. This allows for autonomous high-speed surveys using payload-directed flight methods and on-board pre-processing. At present, both FluidCam 1 (380–720 nm, 3-channel) and FluidCam 2 (300–1100 nm, panchromatic) are being used for UAV-based validation and science missions. In 2016, the entire shoreline of Ofu Island is scheduled to be surveyed as part of an airborne science campaign with FluidCam 1 on a new, payload-directed, multirotor UAV. This upcoming campaign will allow for the first large-scale change detection analysis at centimetre scale in American Samoa by comparison with the preliminary datasets presented here. In addition, an active 5-channel and 36-channel multispectral implementation of FluidCam, called MiDAR, was selected for a NASA CIF 2016 grant. MiDAR operates with an active illumination source and should expand the depth, SNR and ocean surface conditions for which airborne fluid lensing is applicable. Finally, forthcoming publications will present details on fluid lensing methods and validation techniques, as well as results from new machine learning tools developed to semi-autonomously process fluid lensing datasets. These capabilities will enable collection of remote sensing data to quantify coral reef dynamics by documenting reef resilience through percentage cover, morphology and species abundance and distribution.

ACKNOWLEDGEMENTS

This work was supported by NASA Earth Science Technology Office (ESTO) grant ATI-QRS-14-0010. Additional backing was provided by J. Alonso, through a Stanford University Research

Assistantship, and the Aerospace Design Lab (ADL). The Samoa field campaign was supported by J. Pringle and S. Palumbi, Stanford University. In Samoa, PhD students T. Bieri and T. Lukaczyk assisted with flights, underwater data collection and field logistics. The Hamelin Pool airborne campaign was supported and performed in conjunction with R.P. Reid and E.P. Suosaari, University of Miami, RSMAS, whose enthusiasm for stromatolites deterred countless venomous sea-snakes. G. Milano captained the survey boat as a mobile UAV flight deck. Additional Hamelin Pool field support was provided by K. Shaber, J. Foster, A. Shaber-Twedt and E. Karaca. We extend special thanks to C. Caruso, of the National Park Service of American Samoa, and P. Playford, of the Geological Survey of Western Australia for their instrumental roles in permitting these airborne campaigns. P. McGillivary, USCG, and C. Vick, Sylvia Earle Alliance, served a fundamental role as facilitators, coordinators and manuscript editors. We are very grateful to S. Purkis and anonymous reviewers for the invaluable comments. A special thanks to our colleagues at NASA Ames Research Center's Earth Science Division, specifically, R. Instrella, S. Palacios, I. Brosnan, S. Hipskind and D. Alfano for their contributions to this work and A. Michaelis, NASA Earth Exchange (NEX), for advanced supercomputing support. Lastly, we are fortunate to have conducted these surveys over lands protected by the Samoan elders and the aboriginal tribes of Western Australia. Their wisdom, stewardship and conservation of these unique reef ecosystems helped ensure their status as protected marine areas today.

REFERENCES

Aguilar MA, del Mar Saldaña M, Aguilar FJ. 2013. Assessing geometric accuracy of the orthorectification process from GeoEye-1 and WorldView-2 panchromatic images. *International Journal of Applied Earth Observation and Geoinformation* **21**: 427–435.

Baker VR. 2006. Geomorphological evidence for water on Mars. *Elements* **2**: 139–143.

Bannoura WJ, Wade A, Srinivas DN. 2005. NOAA ocean surface topography mission Jason-2 project overview. In *OCEANS, Proceedings of MTS/IEEE;* 2155–2159.

Beijbom O, Edmunds PJ, Roelfsema C, Smith J, Kline DI, Neal BP, Dunlap MJ, Moriarty V, Fan T-Y, Tan C-J, *et al.* 2015. Towards automated annotation of benthic survey images: Variability of human experts and operational modes of automation. *PloS One* **10**: e0130312.

Bellwood DR, Hughes TP, Folke C, Nystrom M. 2004. Confronting the coral reef crisis. *Nature* **429**: 827–833.

Birkeland C, Craig P, Fenner D, Smith L, Kiene WE, Riegl BM. 2008. Geologic setting and ecological functioning of coral reefs in American Samoa. In *Coral Reefs of the USA*. Springer; 741–765.

Brown M, Lowe DG. 2007. Automatic panoramic image stitching using invariant features. *International Journal of Computer Vision* **74**: 59–73.

Burns BP, Goh F, Allen M, Neilan BA. 2004. Microbial diversity of extant stromatolites in the hypersaline marine environment of Shark Bay, Australia. *Environmental Microbiology* **6**: 1096–1101.

Burns J, Delparte D, Gates R, Takabayashi M. 2015. Integrating structure-from-motion photogrammetry with geospatial software as a novel technique for quantifying 3D ecological characteristics of coral reefs. *PeerJ* **3**: e1077.

Canfield DE. 2005. The early history of atmospheric oxygen: homage to Robert M. Garrels. *Annual Review of Earth and Planetary Sciences* **33**: 1–36.

Chirayath V. 2014. Fluid Lensing, applications to high-resolution 3D subaqueous imaging and automated remote biosphere assessment from airborne and space-borne platforms. *AGU Fall Meeting Abstracts* **1**: 1178.

Chirayath V, Instrella R. 2016. Fluid Lensing: Seeing Through Waves. http://www.nasa.gov/ames/las/fluid-lensing-seeing-through-waves

Corson MR, Korwan DR, Lucke RL, Snyder WA, Davis CO. 2008. The Hyperspectral Imager For The Coastal Ocean (HICO) On The International Space Station. In *Geoscience and Remote Sensing Symposium, 2008. IGARSS 2008. IEEE International* IV–101.

Costanza R, D'Arge R, de Groot R, Faber S, Grasso M, Hannon B, Limburg K, Naeem S, O'Neill R, Paruelo J, *et al.* 1997. The value of the world's ecosystem services and natural capital. *Nature* **387**: 253–260.

Debevec PE, Malik J. 1997. Recovering high dynamic range radiance maps from photographs. In *SIGGRAPH'97*; 369–378.

Edinger EN, Limmon G V, Jompa J, Widjatmoko W, Heikoop JM, Risk MJ. 2000. Normal coral growth rates on dying reefs: are coral growth rates good indicators of reef health? *Marine Pollution Bulletin* **40**: 404–425.

Gleyzes M-A, Perret L, Kubik P. 2012. Pleiades system architecture and main performances. *International Archives of the Photogrammetry, Remote Sensing and Spatial Information Sciences* **39**: B1.

Glover L, Earle S. 2004. *Defying Ocean's End: an Agenda for Action*. Island Press: Washington, D.C.

Goodman JA, Purkis SJ, Phinn SR. 2013. *Coral Reef Remote Sensing: A Guide for Mapping, Monitoring and Management*. Springer Science and Business Media.

Google. 2015a. Hamelin Pool. -26.320, 114.232. *Astrium, Pleiades-1A and Google Earth Engine*.

Google. 2015b. Ofu Island. -14.182, −169.658. *Astrium, Pleiades-1A and Google Earth Engine*.

Green RO, Eastwood ML, Sarture CM, Chrien TG, Aronsson M, Chippendale BJ, Faust JA, Pavri BE, Chovit CJ, Solis M, *et al.* 1998. Imaging spectroscopy and the airborne visible/infrared imaging spectrometer (AVIRIS). *Remote Sensing of Environment* **65**: 227–248.

Grotzinger JP, Knoll AH. 1999. Stromatolites in Precambrian carbonates: evolutionary mileposts or environmental dipsticks? *Annual Review of Earth and Planetary Sciences* **27**: 313–358.

Harwin S, Lucieer A. 2012. Assessing the accuracy of georeferenced point clouds produced via multi-view stereopsis from unmanned aerial vehicle (UAV) imagery. *Remote Sensing* **4**: 1573–1599.

Holthuijsen LH. 2010. *Waves in Oceanic and Coastal Waters*. Cambridge University Press: Cambridge, United Kingdom.

Horning N, Robinson J, Sterling E, Turner W, Spector S. 2010. *Remote Sensing for Ecology and Conservation*. Oxford University Press.

Hughes TP, Baird AH, Bellwood DR, Card M, Connolly SR, Folke C, Grosberg R, Hoegh-Guldberg O, Jackson JBC, Kleypas J, *et al*. 2003. Climate change, human impacts, and the resilience of coral reefs. *Science (New York)* **301**: 929–933.

Jahnert R, Collins L. 2012. Characteristics, distribution and morphogenesis of subtidal microbial systems in Shark Bay, Australia. *Marine Geology* **303**: 115–136.

Joyce KE, Belliss SE, Samsonov S V, McNeill SJ, Glassey PJ. 2009. A review of the status of satellite remote sensing and image processing techniques for mapping natural hazards and disasters. *Progress in Physical Geography* **33**: 183–207.

Kanade T, Morris D. 1998. Factorization methods for structure from motion. *Philosophical Transactions of the Royal Society of London A: Mathematical, Physical and Engineering Sciences* **356**: 1153–1173.

Mai T. 2015. Technology Readiness Level. https://www.nasa.gov/directorates/heo/scan/engineering/technology/txt_accordion1.html

Martin S. 2014. *An Introduction to Ocean Remote Sensing*. Cambridge University Press: Cambridge, United Kingdom.

McKay CP, Stoker CR. 1989. The early environment and its evolution on Mars: implication for life. *Reviews of Geophysics* **27**: 189–214.

Moberg F, Folke C. 1999. Ecological goods and services of coral reef ecosystems. *Ecological Economics* **29**: 215–233.

Monismith SG. 2007. Hydrodynamics of coral reefs. *Annual Review of Fluid Mechanics* **39**: 37–55.

Mumby PJ, Skirving W, Strong AE, Hardy JT, LeDrew EF, Hochberg EJ, Stumpf RP, David LT. 2004. Remote sensing of coral reefs and their physical environment. *Marine Pollution Bulletin* **48**: 219–228.

NOAA. 2012. 2012 NOAA American Samoa Lidar: Islands of Tutuila, Aunu'u, Ofu, Olosega, Ta'u and Rose Atoll. NOAA's Ocean Service (NOS), Coastal Services Center (CSC).

Playford PE, Cockbain AE, Berry PF, Roberts AP, Haines PW, Brooke BP. 2013. The geology of Shark Bay. *Geological Survey of Western Australia Bulletin* **146**: 281pp.

Purkis SJ, Riegl B. 2005. Spatial and temporal dynamics of Arabian Gulf coral assemblages quantified from remote-sensing and *in situ* monitoring data. *Marine Ecology Progress Series* **287**: 99–113.

Purkis SJ, Kohler KE, Riegl BM, Rohmann SO. 2007. The statistics of natural shapes in modern coral reef landscapes. *The Journal of Geology* **115**: 493–508.

Purkis SJ, Graham NAJ, Riegl BM. 2008. Predictability of reef fish diversity and abundance using remote sensing data in Diego Garcia (Chagos Archipelago). *Coral Reefs* **27**: 167–178.

Reid RP, Visscher PT, Decho AW, Stolz JF, Bebout BM, Dupraz C, Macintyre IG, Paerl HW, Pinckney JL, Prufert-Bebout L, *et al*. 2000. The role of microbes in accretion, lamination and early lithification of modern marine stromatolites. *Nature* **406**: 989–992.

Ridgwell A, Zeebe R. 2005. The role of the global carbonate cycle in the regulation and evolution of the Earth system. *Earth and Planetary Science Letters* **234**: 299–315.

Rowlands G, Purkis S, Riegl B, Metsamaa L, Bruckner A, Renaud P. 2012. Satellite imaging coral reef resilience at regional scale. A case-study from Saudi Arabia. *Marine Pollution Bulletin* **64**: 1222–1237.

Roy DP, Wulder MA, Loveland TR, Woodcock CE, Allen RG, Anderson MC, Helder D, Irons JR, Johnson DM, Kennedy R, *et al*. 2014. Landsat-8: science and product vision for terrestrial global change research. *Remote Sensing of Environment* **145**: 154–172.

Saul S, Purkis S. 2015. Semi-automated object-based classification of coral reef habitat using discrete choice models. *Remote Sensing* **7**: 15894–15916.

Schlager W, Purkis S. 2015. Reticulate reef patterns - antecedent karst versus self-organization. *Sedimentology* **62**: 501–515.

Spurgeon JPG. 1992. The economic valuation of coral reefs. *Marine Pollution Bulletin* **24**: 529–536.

Suosaari EP, Reid RP, Playford PE, Foster JS, Stolz JF, Casaburi G, Hagan PD, Chirayath V, Macintyre IG, Planavsky NJ, *et al*. 2016. New multi-scale perspectives on the stromatolites of Shark Bay, Western Australia. *Scientific Reports* **6**: 20557.

Tomasi C, Kanade T. 1992. Shape and motion from image streams under orthography: a factorization method. *International Journal of Computer Vision* **9**: 137–154.

UNEP-WCMC. 2010. Global distribution of coral reefs, compiled from multiple sources including the Millennium Coral Reef Mapping Project. UNEP World Conservation Monitoring Centre.

Weinberg S. 1981. A comparison of coral reef survey methods. *Bijdragen tot de Dierkunde* **51**: 199–218.

